UCL Mechanical Engineering 2021/2022

MECH0024 Coursework

RFLH9

December 17, 2021

Contents

I SpaceX rocket engine essay **3**

II Sea Level and Vacuum Merlin 1D rocket engines analysis **5**

1 **5**

1.1 Estimation of ideal OF ratio & comparison with typical value 5

1.2 Estimation of isentropic index γ 6

1.3 Estimation of molecular weight of combustion products M_g 6

1.4 Estimation of heat capacity c_p 7

1.5 Estimation of the adiabatic flame temperature of the combustion product in the combustion chamber 7

2 Determination of mass flux through both rocket engines **8**

3 Estimation of exit velocity of jet exhaust in both cases **8**

4 Estimation of exit pressure of the exhaust in both cases **9**

5 **10**

5.1 Estimation of rocket thrust for the Sea Level Merlin 1D during the initial take-off and the Vacuum Merlin 1D operating in space 10

5.2 Estimation of the specific impulse in both cases 11

5.3 Discussion of differences between estimations and reported values 12

6 Sketch of exit flow/shock expansion fan characteristics 12

6.1 At sea level . . . 12

6.2 At an altitude of 5.5 km . . . 14

7 Description of other technologies (and their working principles), which accommodate the change in back-pressure on thrust performance 15

List of Figures

1 Open-cycle gas-generator cycle [2]. . . . 3

2 Merlin engine test fire. Note the sooty exhaust on the right side from the preburner and turbine [3]. 3

3 Closed-cycle staged combustion cycle [5]. . . . 4

4 Full-flow staged combustion cycle [6]. . . . 4

5 Isentropic index γ vs. Chamber pressure P_c (atm) for Kerosone. . . . 6

6 Gas Molecular Weight M_g ($\mathrm{g\,mol^{-1}\,K^{-1}}$) vs. Chamber pressure P_c (atm) for Kerosene. . . . 6

7 Adiabatic Flame Temperature T_P (K) vs. Chamber pressure P_c (atm) for Kerosene. . . . 7

8 Sketch of over-expanded flow with regular shocks. . . . 13

9 Sketch of over-expanded flow with regular shocks at the nozzle boundary. . . . 13

10 Sketch of over-expanded flow with regular shocks at the expansion fan. . . . 13

11 Sketch of over-expanded flow with regular shocks. . . . 14

12 Sketch of over-expanded flow with regular shocks at the nozzle boundary. . . . 14

13 Aerospike in high and low back-pressure environments. . . . 15

List of Tables

1 Exit velocities of vacuum and sea level Merlin 1D engines. . . . 9

2 Exit pressures of vacuum and sea level Merlin 1D engines. . . . 10

3 Thrust of vacuum and sea level Merlin 1D engines. . . . 11

4 Thrust of vacuum and sea level Merlin 1D engines. . . . 12

5 Thrust of vacuum and sea level Merlin 1D engines. . . . 12

Part I

SpaceX rocket engine essay

SpaceX has been developing rocket engines for nearly two decades. The two primary engine families being developed today are the Merlin series and the Raptor series. The Draco and SuperDraco series of engines have also been developed by SpaceX, however their role as Reaction Control System (RCS) thrusters and Launch Abort System engines respectively leave them to be not considered in this essay. SpaceX has developed these rocket engines to power a variety of booster rockets, including the Falcon 9, Falcon Heavy and Starship. The roles of these rockets include delivering crew and cargo to space, as well as interplanetary travel. SpaceX places a strong emphasis on reusability and a reduction of ‘cost to launch’. Hence, the engines powering these flights must be efficient, powerful and reliable to facilitate multiple missions.

The Merlin series powers the Falcon 9 and Falcon Heavy rocket boosters. These are two-stage rockets, designed to place cargo and crew into earth orbit. The first stage is powered by nine Merlin ‘sea level’ engines and the second stage is powered by one Merlin ‘vacuum’ engine. There have been a variety of developments over the past years and the current generation of Merlin engines is the Merlin 1D. The Merlin 1D uses an open-cycle gas-generator cycle with Rocket Propellant 1 (RP-1) and liquid oxygen (LOX) as propellants.

The fuel choice for the Merlin engine is due to a large variety of factors. The Merlin engine uses liquid propellants for combustion. RP-1 is a refined kerosene with low amounts of impurities and has been a widely used choice for the past 70 years. It is a liquid at room temperature, safe to handle, cheap and available in large quantities. This makes it ideal for rockets which need to fly frequently (as the Falcon rockets do). However, RP-1 is not the most efficient fuel as liquid Hydrogen (LH2) has a far greater specific impulse (289 s vs 381 s) but RP-1 has greater density ($0.071\,\mathrm{g\,mol^{-1}}$ vs $0.82\,\mathrm{g\,mol^{-1}}$) [1]. Another disadvantage of RP-1 is that it is a hydrocarbon, resulting in carbon deposits when burnt at the improper fuel-oxidiser ratio. This can lead to a build up of carbon deposits in the engine, decreasing the lifetime of the engine. Some alternatives to RP-1 include LH2 and liquid Methane. These two fuels are sometimes referred to as cryogenic fuels as their boiling points are far below room temperature and require more complex pressurised tanks and plumbing within the engine, presenting a different set of engineering challenges. After passing through the turbopumps, the propellants are driven through a pintle type injector and combusted in the main chamber.

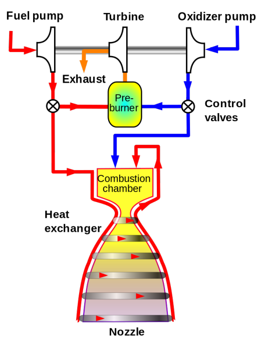

Figure 1: Open-cycle gas-generator cycle [2].

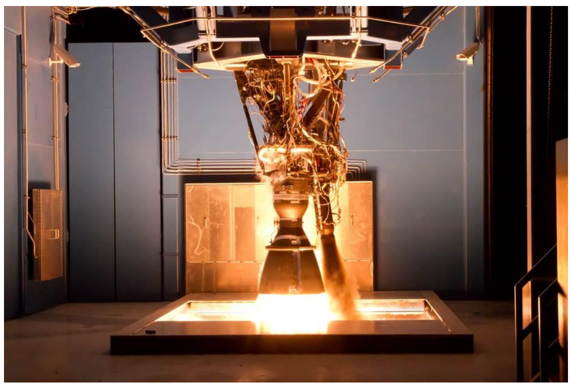

Figure 2: Merlin engine test fire. Note the sooty exhaust on the right side from the preburner and turbine [3].

To dissect the combustion cycle of the Merlin engine, let us take a look at how the engine is designed. In Figure 1, we see that RP-1 and LOX is fed through turbopumps powered by a turbine on a single shaft. The turbine is driven by hot gas from a ‘preburner’. Some of the fuel and oxidiser is tapped off before it reaches the main combustion chamber for preburner combustion. After passing through the turbine, the gas is exhausted overboard. We see this as the sooty exhaust in Figure 2. The presence of soot in the preburner exhaust is evidence of a fuel rich fuel-oxidiser ratio. As the combustion products from the preburner are not used in the main combustion chamber, we have a definitive loss in efficiency as we are not utilising all of our fuel for main engine thrust. We refer to this as an ‘open-cycle’. Another issue to contend with is shaft leak. This is where the fuel rich gas from the preburner can seep through the shaft interpropellant seal towards the oxidiser turbopump. This may cause combustion before the propellants reach the main combustion chamber, reducing efficiency.

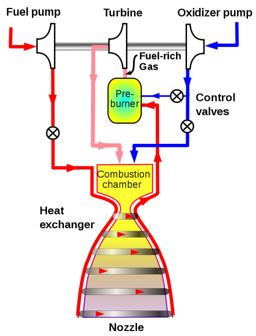

Figure 3: Closed-cycle staged combustion cycle [5].

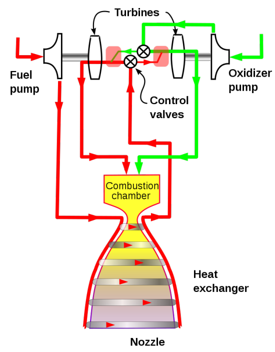

Figure 4: Full-flow staged combustion cycle [6].

To improve the efficiency of this cycle, we can feed the exhaust from the turbine into our main combustion chamber 'closing our cycle'. This is also called a staged combustion cycle and Figure 3 shows a general closed-cycle staged combustion cycle. This presents an engineering problem as the main combustion chamber will exert pressure back through to the turbine and pre-burner. To solve this problem, the preburner needs to generate more energy and higher pressures to better match the pressure within the main combustion chamber. The turbine will need to withstand higher temperatures and larger stresses, requiring advanced metallurgy. The Merlin engine reduces the stress on its turbine by running fuel rich as this reduces the combustion temperature. As our fuel is hydrocarbon based, we run the risk of 'coking' where carbon deposits clog the plumbing within the engine. We can run our preburner oxidiser rich (e.g. NPO Energomash RD-180 engine [4]) but this results in an exhaust which is chemically corrosive, due to the presence of high temperature oxygen. Higher pressures and temperatures will also exacerbate our shaft leak problem, requiring tighter engineering tolerances. Closed-cycle staged combustion cycle engines are more efficient but have more complex designs, leading to added weight and an increased cost to manufacture and maintain. A balance must be struck to ensure that these engines are viable.

The SpaceX Raptor engine utilises a full-flow staged combustion cycle (Figure 4) with liquid Methane and liquid Oxygen as propellants. This is the first engine of its kind to propel a rocket. Liquid Methane has a higher specific impulse than RP-1 but still not as high as LH2 [1]. Similar to RP-1, liquid Methane is more dense than LH2 and can be cryonically stored in the tanks to increase volume of fuel onboard. As Methane is a smaller hydrocarbon than kerosene, it burns much cleaner, reducing the effect of the coking problem with RP-1. It is also abundant and can be easily made on other planets.

In the full-flow design, we see two separate turbines powering each turbopump. This separates our fuel-rich and oxidiser-rich gases, eliminating the need for interpropellant seals along our shafts. This design requires less energy per turbine as it only has to power one turbompump, leading to cooler preburner temperatures. This improves turbine life and reliability. By the time the propellants reach the combustion chamber, the propellants are gases, due to heating from the preburners. Gaseous propellants improve efficiency as you no longer have to force liquid propellants through an injector (which takes energy away from the propellants); the gases can mix very rapidly and efficiently in the main chamber. We also see higher mass flow rates as all the fuel and oxidiser is used in the main combustion chamber. This allows for a reduction in the pressures required, leading to even lower temperatures and lower stresses on the engine, improving reusability. The full-flow cycle is even more complex than the closed-cycle, as each preburner is reliant on the other. This requires precise engine control and a fast start-up sequence of both preburners to prevent an imbalance in fuel/oxidiser ratio.

A novel design of the SpaceX engines is the use of subcooled propellants. When the propellants are closer to their freezing points, their densities are higher. When passing the propellants through the turbopumps, we may see cavitation at the tips of the impeller blades if the propellant is close to its boiling point (due to high pressures). By subcooling the propellant, we can lower our RPM and still deliver the same mass flow rate (due to higher propellant density). This reduces the risk of cavitation as a lower tip speed will lead to a lower pressure differential, decreasing the risk of cavitation. The Raptor engine heavily incorporates 3D printed components. An estimated 40% of the components on the Raptor engine are 3D printed [7]. Both Merlin and Raptor engines use components which are heavily vertically integrated within SpaceX. Compared to rocket engines built by other manufacturers, where components are built by numerous contractors, SpaceX engine components are almost all designed and built in-house, reducing cost and allowing for a high level of customisability.

All of these developments allow for SpaceX engines to be reliable and powerful, having been used and reused many times on Falcon and Starship rocket flights.

Part II

Sea Level and Vacuum Merlin 1D rocket engines analysis

1

1.1 Estimation of ideal OF ratio & comparison with typical value

Using Kerosene and Oxygen as our propellants, our chemical balance is:

$$C_{12}H_4 + 36\,O_2 \longrightarrow 12\,H_2O + 12\,CO_2 \tag{1.1}$$

Therefore, stoichiometric oxidiser-fuel ratio by mass is:

$$\mathrm{OF}_{stoi} = \frac{18(32\,\mathrm{g\,mol^{-1}})}{12(12\,\mathrm{g\,mol^{-1}}) + 24(1\,\mathrm{g\,mol^{-1}})} = \frac{576}{168} = 3.429 \tag{1.2}$$

A typical oxidiser-fuel ratio for RP-1 LOX rocket engines is given as $\mathrm{OF}_{typ} = 2.3$. This tells us that these engines run fuel rich. Richard Nakka derives 1.3 [8]:

$$v_e = \sqrt{2T_0\left(\frac{R'}{M}\right)\left(\frac{k}{k-1}\right)\left[1-\left(\frac{P_e}{P_0}\right)^{\frac{k-1}{k}}\right]} \tag{1.3}$$

where:

- v_e is the exit velocity at the nozzle of the engine.
- T_0 is the combustion temperature of propellant.
- $R' = 8314\,\mathrm{J\,kmol^{-1}\,K^{-1}}$ is the universal gas constant.
- M is the effective molecular weight of exhaust products.
- k effective ratio of specific heats of exhaust products.
- P_e is nozzle exit pressure.
- P_0 is chamber pressure.

Here we can see that if we decrease the molecular weight of our exhaust, we increase our nozzle velocity. This makes it desirable to have lighter exhaust products. In the case of RP-1 LOX combustion, it would be preferable to have CO mixed into our exhaust alongside H_2O and CO_2, as this would reduce the overall molecular weight of the exhaust. Running fuel rich ensures that all of the oxygen is used for combustion, increasing overall efficiency. We must be careful to fine tune our OF ratio, as running too fuel rich may leave unburnt kerosene in the exhaust (which is relatively heavy). Even the partial combustion to CO is less energetic and too much CO in the exhaust will lead to inefficiency.

We may also want to run fuel rich to lower our combustion temperature. If our combustion temperature is too hot, we risk damaging components in the engine. It also ensures that we do not have unburned, hot oxidiser (which is corrosive towards metals) damaging engine components.

1.2 Estimation of isentropic index γ

Chamber pressure of Merlin 1D engine is given as 9.7 MPa. Converting to standard atmospheres:

$$P_c = 9.7\,\text{MPa} = 95.7\,\text{atm} \tag{1.4}$$

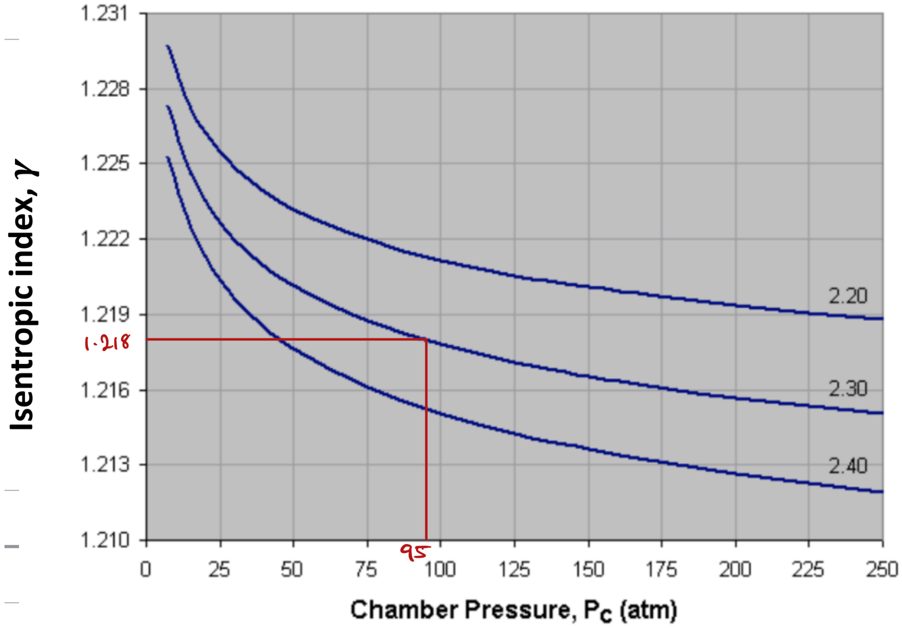

Figure 5: Isentropic index γ vs. Chamber pressure P_c (atm) for Kerosone.

Estimating the value from Figure 5:

$$\gamma \approx 1.218 \tag{1.5}$$

1.3 Estimation of molecular weight of combustion products M_g

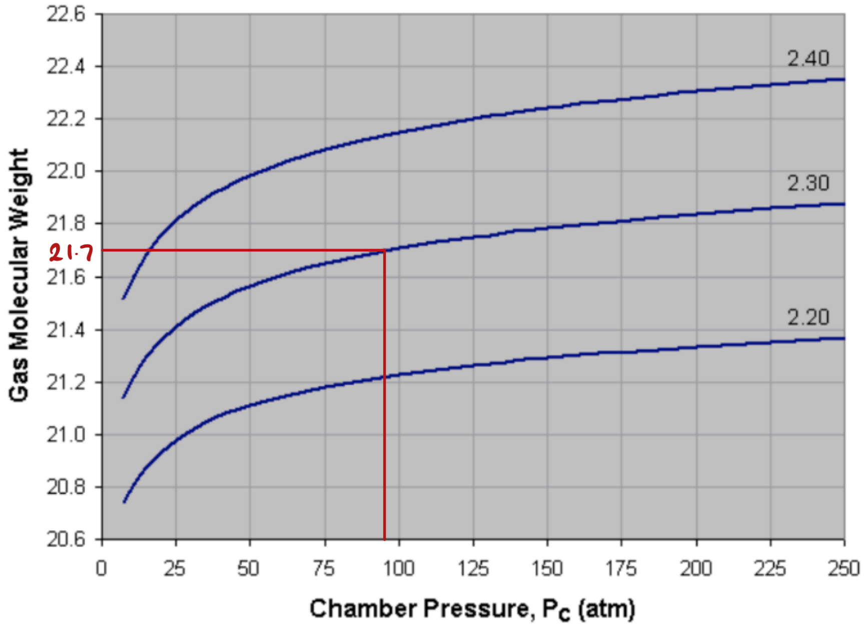

Figure 6: Gas Molecular Weight M_g ($\text{g}\,\text{mol}^{-1}\,\text{K}^{-1}$) vs. Chamber pressure P_c (atm) for Kerosene.

Estimating the value from Figure 6:

$$M_g \approx 21.7\,\mathrm{g\,mol^{-1}} \tag{1.6}$$

1.4 Estimation of heat capacity c_p

We know that:

$$\gamma = \frac{C_p}{C_v} \tag{1.7}$$

$$C_p - C_v = R' \tag{1.8}$$

where $R' = 8.31\,\mathrm{J\,mol^{-1}\,K^{-1}}$. Therefore:

$$C_v = C_p - R' \tag{1.9}$$

$$\gamma = \frac{C_p}{C_p - R'} \tag{1.10}$$

Rearranging for C_p:

$$C_p = \frac{\gamma R'}{\gamma - 1} \tag{1.11}$$

Using values estimated previously:

$$C_p = \frac{1.218(8.31\,\mathrm{J\,mol^{-1}\,K^{-1}})}{1.218 - 1} \tag{1.12}$$

$$C_p = 46.34\,\mathrm{J\,mol^{-1}\,K} \tag{1.13}$$

1.5 Estimation of the adiabatic flame temperature of the combustion product in the combustion chamber

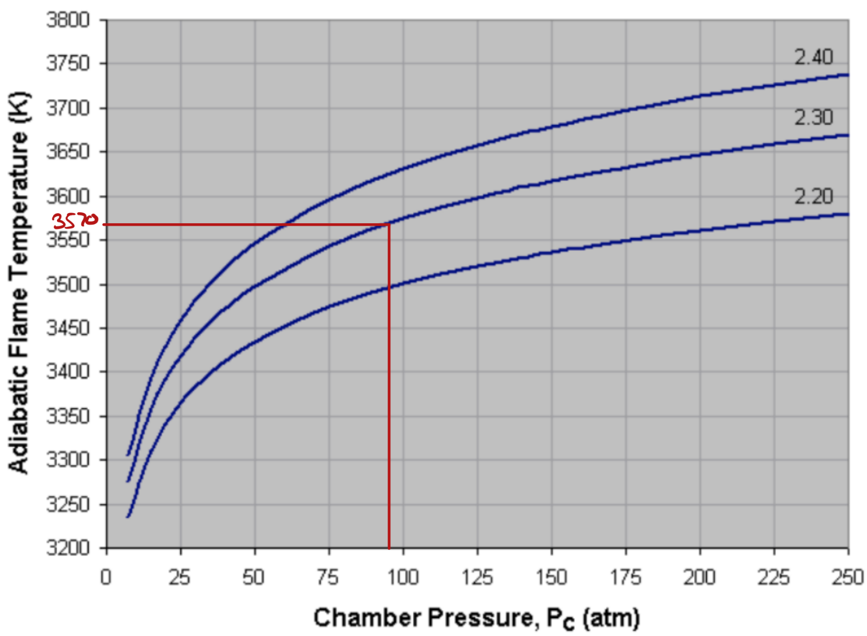

Figure 7: Adiabatic Flame Temperature T_P (K) vs. Chamber pressure P_c (atm) for Kerosene.

Estimating the value from Figure 7:

$$T_P = 3570\,\mathrm{K} \tag{1.14}$$

2 Determination of mass flux through both rocket engines

Here, we can model the system as a duct flow and we can utilise the critical state conditions (denoted with '*'). We can also use $M = 1$ as the sonic condition is met. Conservation of mass dictates that:

$$\dot{m} = \rho u A = \rho^* u^* A^* = \text{const} \tag{2.1}$$

$$\frac{\rho}{\rho^*}\frac{u}{u^*}\frac{A}{A^*} = 1 \tag{2.2}$$

We can assume the flow is isentropic, therefore:

$$\frac{\rho}{\rho^*} = \left(\frac{1+\frac{1}{2}(\gamma-1)M^2}{\frac{1}{2}(\gamma+1)}\right)^{-\frac{1}{\gamma-1}} \tag{2.3}$$

We can assume the flow is adiabatic, therefore:

$$\frac{u}{u^*} = M\left(\frac{\frac{1}{2}(\gamma+1)}{1+\frac{1}{2}(\gamma-1)M^2}\right)^{\frac{1}{2}} \tag{2.4}$$

The mass flux (per unit area) is $\frac{m}{A} = \rho u$. Its derivate w.r.t. M is:

$$\frac{\mathrm{d}}{\mathrm{d}M}\left(\frac{\rho u}{\rho_* u_*}\right) = \left(1-M^2\right)\left(1+\frac{1}{2}(\gamma-1)M^2\right)^{-\frac{\gamma-3}{2(\gamma-1)}}\left(\frac{1}{2}(\gamma+1)\right)^{\frac{\gamma+1}{2(\gamma-1)}} \tag{2.5}$$

Maximum occurs when $M = 1$, when the flow is choked. The maximum mass flux is:

$$\dot{m}_{max} = \rho^* u^* A^* = \left(\frac{2}{\gamma+1}\right)^{\frac{\gamma+1}{2(\gamma-1)}}\sqrt{\frac{\gamma}{RT_0}}A^* p_0 \tag{2.6}$$

Where p_0 is the chamber pressure. We know the diameter of our throat:

$$A^* = \left(\frac{0.226}{2}\right)^2 \pi\, \mathrm{m}^2 \tag{2.7}$$

Hence, mass flow rate is:

$$\dot{m}_{max} = \left(\frac{2}{1.218+1}\right)^{\frac{1.218+1}{2(1.218-1)}}\sqrt{\frac{1.218}{\left(\frac{8314}{21.7}\right)(3570)}}\left(\left(\frac{0.226}{2}\right)^2\pi\right)\left(9.7\times10^6\right) \tag{2.8}$$

$$\dot{m}_{max} = 216.93\,\mathrm{kg\,s^{-1}} \tag{2.9}$$

The sea level and vacuum variants of the Merlin 1D have the same throat area, hence they have the same mass flow rate.

3 Estimation of exit velocity of jet exhaust in both cases

Exit velocity is given by the following equation:

$$u_e = M_e\sqrt{\gamma R T_c\left(1+\frac{1}{2}(\gamma-1)M_e^2\right)^{-1}} \tag{3.1}$$

Exit Mach number is related to the throat and nozzle areas by:

$$\frac{A_e}{A_t} = \frac{1}{M_e}\left(\frac{1+\frac{1}{2}(\gamma-1)M_e^2}{\frac{1}{2}(\gamma+1)}\right)^{\frac{\gamma+1}{2(\gamma-1)}} \tag{3.2}$$

Using MATLAB, the values for the exit Mach number for the vacuum and sea level Merlin 1D engine was calculated. This was then used to calculate the exit velocity:

```
clc
clear
close all

%define constants
gamma = 1.218;
d = [3.31 0.92]; %vacuum and sea level exit nozzle diameters
At = ((0.226/2)^2)*pi; %throat diameter
R = 8173/21.7;
Tc = 3570;


%initialise arrays and variables
eqn = zeros(1,2);
MachE = zeros(1,2);
ue = zeros(1,2);
syms Me

%solve for exit Mach number
for i = 1:2
    Ae = ((d(i)/2)^2)*pi;
    eqn = (1/Me)*((1 + 0.5*(gamma
        -1)*(Me^2))/(0.5*(gamma + 1)))^((gamma +1)/(2*(gamma - 1))) == Ae/At;
    MachE(i) = vpasolve(eqn, Me);
end

%solve for exit velocity
ue = MachE.*sqrt(gamma*R*Tc*(1 + 0.5*(gamma -1).*(MachE.^2)).^(-1));
```

Engine Variant	Exit velocity u_e / $\mathrm{m\,s^{-1}}$
Vacuum	3416
Sea level	2999

Table 1: Exit velocities of vacuum and sea level Merlin 1D engines.

4 Estimation of exit pressure of the exhaust in both cases

The equation relating exit pressure, main chamber pressure and Mach number is:

$$\frac{p_e}{p_c} = \left(1 + \frac{1}{2}\left(\gamma - 1\right) M_e^2\right)^{-\frac{\gamma}{\gamma-1}} \tag{4.1}$$

Using MATLAB, the values for the exit pressure for the vacuum and sea level Merlin 1D engines was calculated.

```
clc
clear
close all

%define constants
gamma = 1.218;
d = [3.31 0.92]; %vacuum and sea level exit nozzle diameters
At = ((0.226/2)^2)*pi; %throat diameter
pc = 9.7e6;


```

```
%initialise arrays and variables
eqn = zeros(1,2);
MachE = zeros(1,2);
pe = zeros(1,2);
syms Me

%solve for exit Mach number
for i = 1:2
    Ae = ((d(i)/2)^2)*pi;
    eqn = (1/Me)*((1 + 0.5*(gamma
        -1)*(Me^2))/(0.5*(gamma + 1)))^((gamma +1)/(2*(gamma - 1))) == Ae/At;
    MachE(i) = vpasolve(eqn, Me);
end

%solve for exit pressure
pe = pc.*(1 + 0.5*(gamma - 1).*MachE.^2).^(-((gamma)/(gamma - 1)));
```

Engine Variant	Exit pressure p_e / Pa
Vacuum	2235.2
Sea level	59261.2

Table 2: Exit pressures of vacuum and sea level Merlin 1D engines.

5

5.1 Estimation of rocket thrust for the Sea Level Merlin 1D during the initial take-off and the Vacuum Merlin 1D operating in space

Rocket thrust is given by the following equation:

$$F = \dot{m}u_e + (p_e - p_b)\,A_e \tag{5.1}$$

where p_b is the back pressure. At sea level, our back pressure is the atmosphere pressure at sea level, given as 101 325 Pa. In the vacuum of space, our back pressure is negligible and can be taken to be 0 Pa. Using MATLAB, the values for the thrust in each case was calculated.

```
clc
clear
close all

%define constants
gamma = 1.218;
d = [3.31 0.92]; %vacuum and sea level exit nozzle diameters
At = ((0.226/2)^2)*pi; %throat diameter
pc = 9.7e6;
R = 8173/21.7;
Tc = 3570;
mdot = 216.93;

%initialise arrays and variables
eqn = zeros(1,2);
MachE = zeros(1,2);
pe = zeros(1,2);
pb = [0 101325];
F = zeros(1,2);
```

```
syms Me

%solve for exit Mach number
for i = 1:2
    Ae = ((d(i)/2)^2)*pi;
    eqn = (1/Me)*((1 + 0.5*(gamma -1)*(Me^2))/(0.5*(gamma + 1)))^((gamma +1)/(2*(gamma - 1))) == Ae/At;
    MachE(i) = vpasolve(eqn, Me);
end

%solve for exit pressure
pe = pc.*(1 + 0.5*(gamma - 1).*MachE.^2).^(-((gamma)/(gamma - 1)));

%solve for exit velocity
ue = MachE.*sqrt(gamma*R*Tc*(1 + 0.5*(gamma -1).*(MachE.^2)).^(-1));

%initialise array
Ae = zeros(1,2);
%thrust
for i = 1:2
    Ae(i) = ((d(i)/2)^2)*pi;
    F(i) = mdot*ue(i) + (Ae(i))*(pe(i)-pb(i));
end
```

Scenario	Thrust F / N
Vacuum Merlin 1D in Space	760273
Sea level Merlin 1D at Sea Level	622528

Table 3: Thrust of vacuum and sea level Merlin 1D engines.

5.2 Estimation of the specific impulse in both cases

Specific impulse is given by the following equation:

$$I_{sp} = \frac{F}{\dot{m}g} \tag{5.2}$$

Using MATLAB, the value for specific impulse in each case was calculated.

```
clc
clear
close all

%define constants
F = [760272.966085493,622528.049680715];
mdot = 216.93;
g = 9.81;

%initialise array
ISp = zeros(1,2);

%specific impulse
for i = 1:2
    ISp(i) = (F(i))/(mdot*g);
end
```

Scenario	Specific Impulse I_{sp} / s
Vacuum Merlin 1D in Space	357.2
Sea level Merlin 1D at Sea Level	292.5

Table 4: Thrust of vacuum and sea level Merlin 1D engines.

5.3 Discussion of differences between estimations and reported values

Scenario	Thrust F / N	Specific Impulse I_{sp} / s
Vacuum Merlin 1D in Space		
Calculated values	760273	357.2
Reported values	981000	311
Sea level Merlin 1D at Sea Level		
Calculated values	622528	292.5
Reported values	854000	282

Table 5: Thrust of vacuum and sea level Merlin 1D engines.

We see that our calculated values for thrust are lower than the reported values. We also see that our calculated values for specific impulse are higher than the reported values. This may be due to the fact that our mass flow rate of propellant is not correct. If we increase the mass flux of propellant, our thrust would increase and specific impulse decrease. The Merlin engines may require a higher mass flow rate due to losses. We have also assumed that our flow is isentropic and adiabatic, when this may not be the case in reality.

Our exit pressures may also be off. As the rocket flies through the air, the back-pressure drops. Hence, it makes sense to optimise the exit pressure to be as low as possible to maximise the thrust from the first stage. Lowering the exit pressure too much on the sea level engines will result in over-expansion at the nozzle tips and flow separation. This would decrease the efficiency significantly.

6 Sketch of exit flow/shock expansion fan characteristics

6.1 At sea level

At sea level, our back-pressure is 101 325 Pa. Our $\frac{p_b}{p_e}$ ratio can be calculated as:

$$\frac{p_b}{p_e} = \frac{101325}{59261} = 1.71 \tag{6.1}$$

This tells us that our flow will be over-expanded with regular shocks.

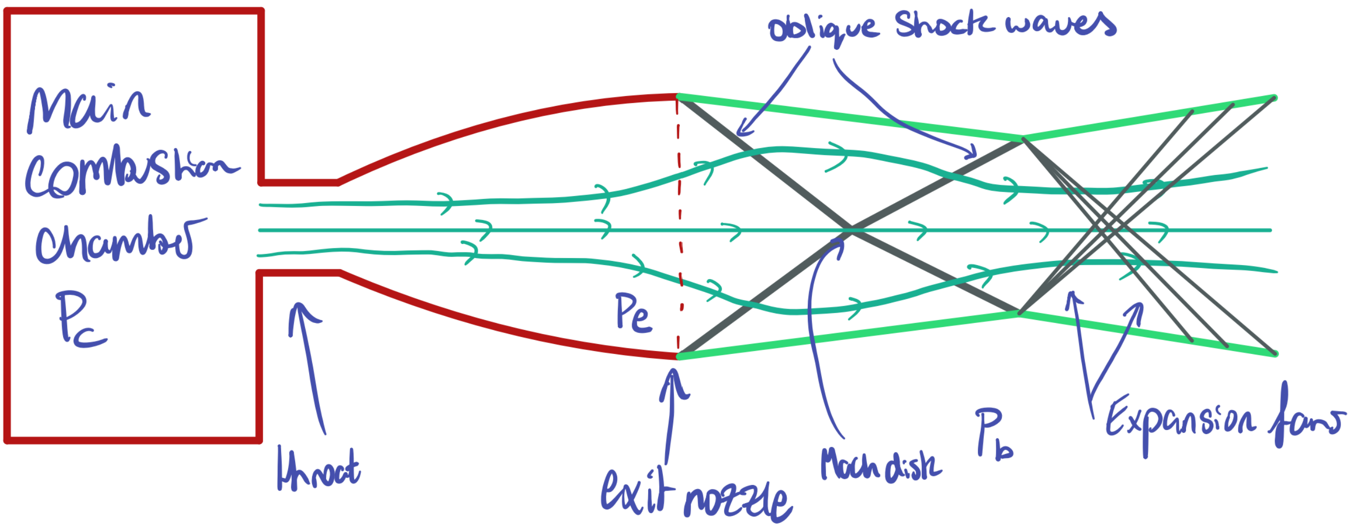

Figure 8: Sketch of over-expanded flow with regular shocks.

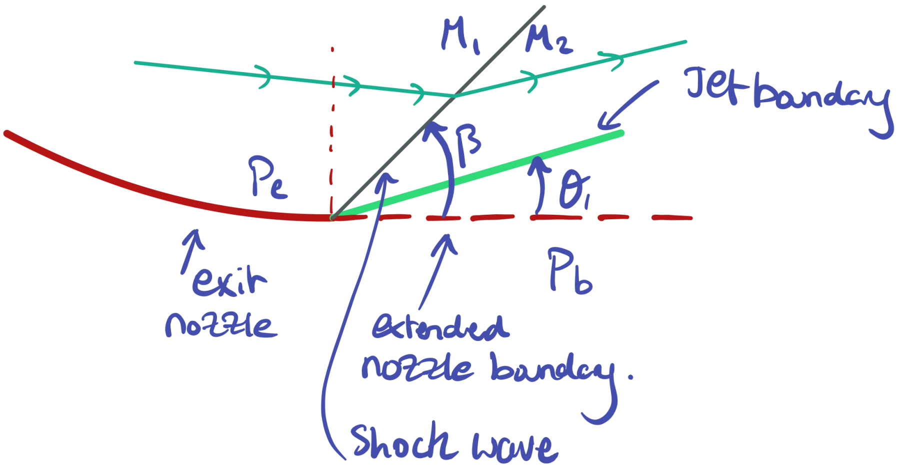

Figure 9: Sketch of over-expanded flow with regular shocks at the nozzle boundary.

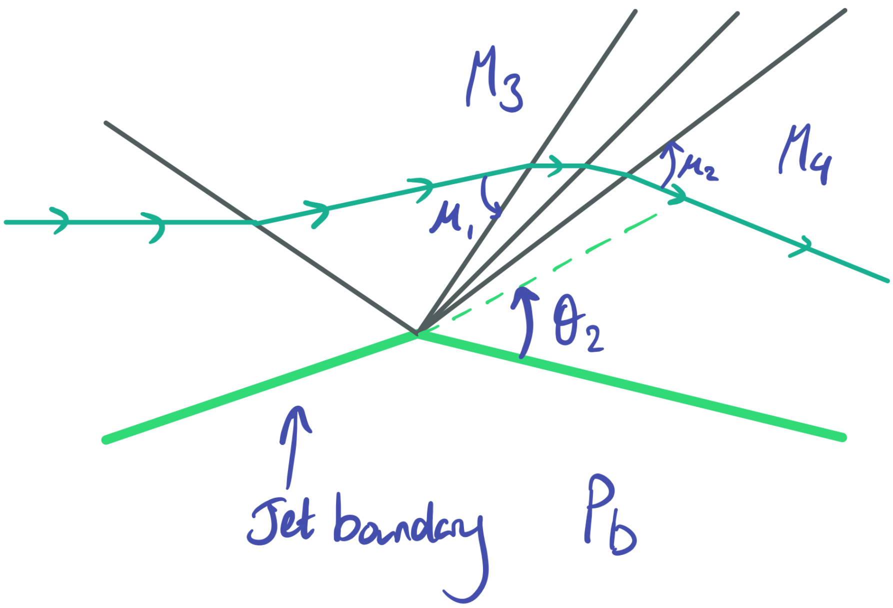

Figure 10: Sketch of over-expanded flow with regular shocks at the expansion fan.

6.2 At an altitude of 5.5 km

At an altitude of 5.5 km, our back-pressure can be calculated by the general barometric formula:

$$P = P_{atm} e^{-\frac{Mgh}{RT}} \tag{6.2}$$

Inputting our constants, $T = 300\,\mathrm{K}$ and $h = 5500\,\mathrm{m}$:

$$P = 101325 \cdot e^{-\dfrac{28.96 \cdot 9.81 \cdot 5500}{8.314 \cdot 300}} = 54163.5 \tag{6.3}$$

Our $\frac{p_b}{p_e}$ ratio can be calculated as:

$$\frac{p_b}{p_e} = \frac{54163.5}{59261} = 0.91 \tag{6.4}$$

This tells us that our flow will be under-expanded with expansion fans.

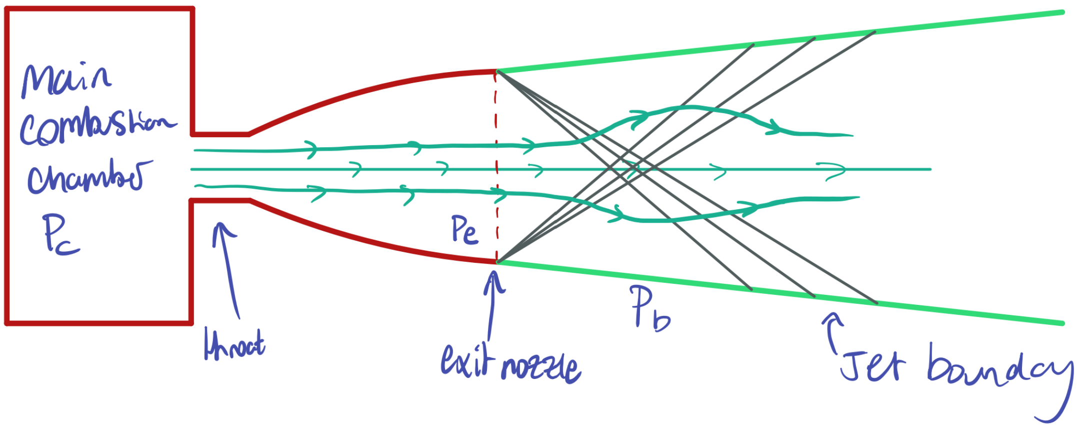

Figure 11: Sketch of over-expanded flow with regular shocks.

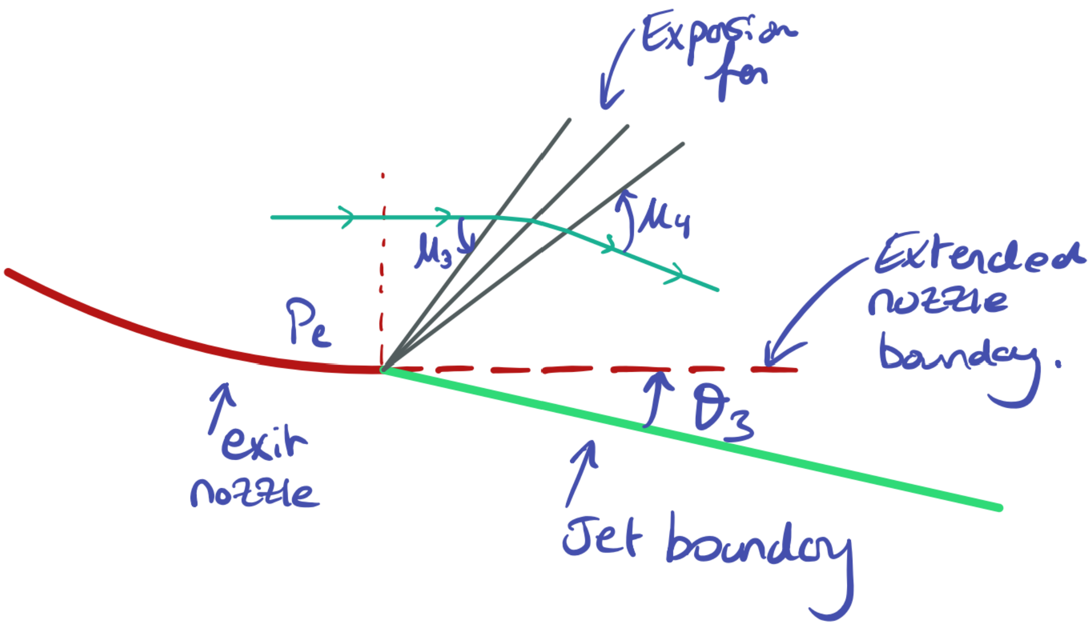

Figure 12: Sketch of over-expanded flow with regular shocks at the nozzle boundary.

7 Description of other technologies (and their working principles), which accommodate the change in back-pressure on thrust performance

A departure from traditional designs, the aerospike claims to be able to solve the issue of fixed exit areas. The basic design involves a number of smaller engines and the curve of a bell nozzle, usually arranged as a wedge or as a radial 'spike'. By allowing the atmosphere to push against the jet boundary, we eliminate our flow separation problem completely. As the pressure drops, our flow becomes wider, automatically compensating. However, aerospikes have been shown to be incredibly difficult to cool appropriately. Common methods such as regenerative and radiative cooling are more difficult to implement. Using more heat resistant alloys adds weight, and this is another area where aerospikes struggle. Aerospikes are typically larger and have worse thrust to weight ratios. This also makes them harder to gimbal on a rocket. All in all, if aerospikes can be made lighter and more compact, they represent a more efficient engine within the atmosphere.

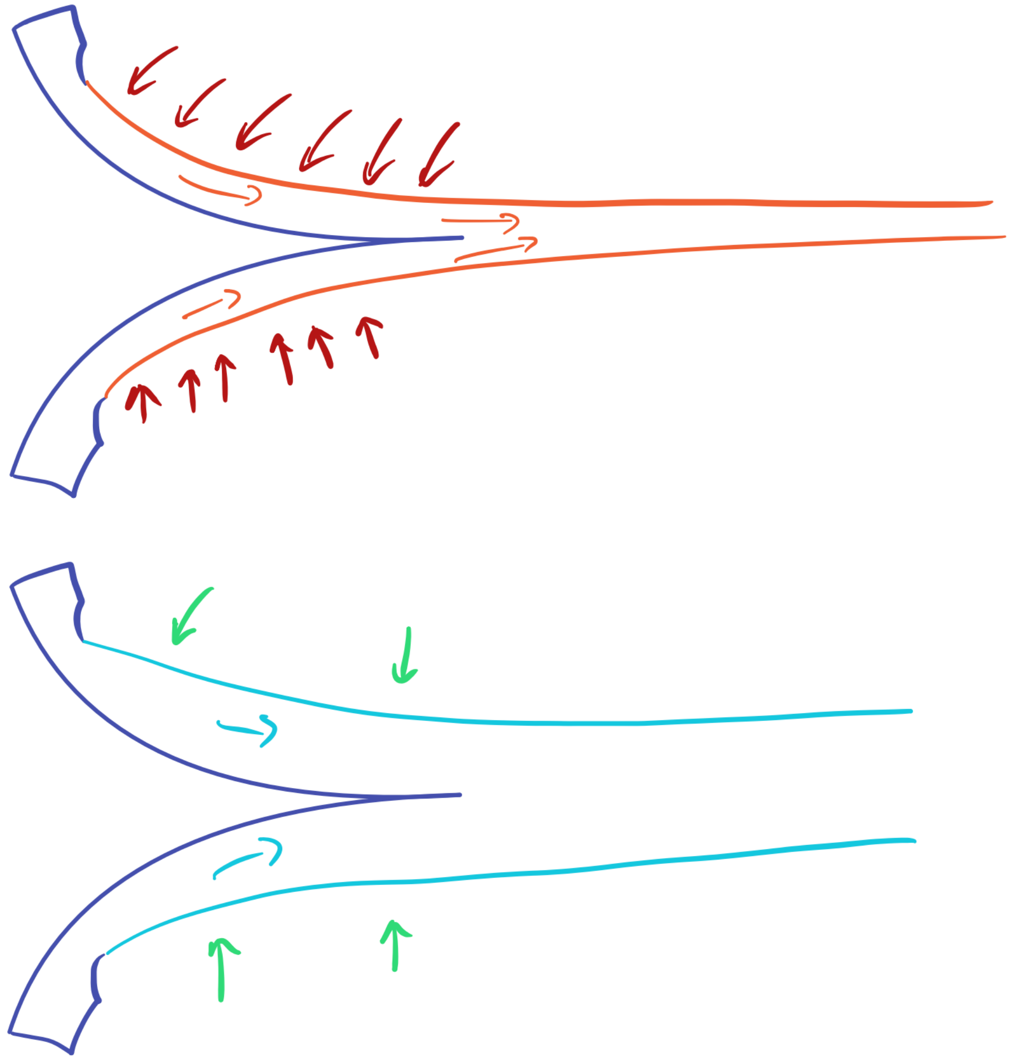

Figure 13: Aerospike in high and low back-pressure environments.

[9]

References

[1] Robert A. Braeunig, (2008) 'Rocket Propellants' http://www.braeunig.us/space/propel.htm Accessed: 14/12/2021

[2] Duk, (2016) 'Gas Generator Rocket Cycle' https://commons.wikimedia.org/wiki/File:Gas_generator_rocket_cycle.svg; see also https://commons.wikimedia.org/wiki/User:Duk, CC BY-SA 3.0, Accessed 15/12/2021

[3] SpaceX. (2012) 'Merlin 1D Test Fire' http://www.spacex.com/media-gallery/detail/1661/172; see also http://www.spacex.com/news/2013/03/26/merlin-engines, CC0, https://commons.wikimedia.org/w/index.php?curid=46487822 Accessed: 15/12/2021

[4] Mark Wade, (2019) 'RD-180' http://www.astronautix.com/r/rd-180.html Accessed: 15/12/2021

[5] Duk, (2017) 'Staged Combustion Cycle' https://commons.wikimedia.org/wiki/File:Staged_combustion_rocket_cycle.svg#filelinks; see also https://commons.wikimedia.org/wiki/User:Duk, CC BY-SA 3.0, Accessed 15/12/2021

[6] Duk, (2021) 'Staged Combustion Cycle' https://commons.wikimedia.org/wiki/File:Full_flow_staged_rocket_cycle.svg; see also https://commons.wikimedia.org/wiki/User:Duk, CC BY-SA 3.0, Accessed 15/12/2021

[7] Alejandro G. Belluscio, (2016) 'The evolution of the SpaceX Raptor engine' https://www.nasaspaceflight.com/2016/10/its-propulsion-evolution-raptor-engine/ Accessed: 15/12/2021

[8] Richard Nakka, (2015) 'Solid Rocket Motor Theory – Nozzle Theory' http://www.nakka-rocketry.net/th_nozz.html Accessed: 15/12/2021

[9] Tim Dodd, (2019) 'Are Aerospike Engines Better Than Traditional Rocket Engines?' https://everydayastronaut.com/aerospikes/ Accessed 17/12/2021